Ral GTPase Activation by Downregulation of RalGAP Enhances OSCC Progression

P. Gao, S. Liu, R. Yoshida, C.Y. Shi, S. Yoshimachi, N. Sakata, K. Goto, T. Kimura, R. Shirakawa, H. Nakayama, J. Sakata, S. Kawashiri, K. Kato, X.Y. Wang, and H. Horiuchi

Appendix

Appendix Table 1. Antibodies for immunoblot and immunoprecipitation

Antibody	Company	M.W. (kDa)	Host	polyclonal/ monoclonal	catalogue number
RalA	BD Transduction Laboratories (San Jose, CA, USA)	28	Mouse	mono	610222
RalB	Cell Signaling (Danvers, MA, USA)	26	Rabbit	poly	3523S
Ras	Millipore (Burlington, MA, USA)	21	Mouse	mono	05-516
GAPDH	Wako Pure Chemical Industries, Ltd. (Osaka, Japan)	38	Mouse	mono	/
RalGAPα1	Made by ourselves previously (Shirakawa et al. 2009)	260/240	Rabbit	poly	/
RalGAPα2	Made by ourselves previously (Saito et al. 2013)	220	Rabbit	poly	/
RalGAPβ	Made by ourselves previously (Shirakawa et al. 2009)	170	Rabbit	poly	/
H3	Abcam (Cambridge, UK)	17	Rabbit	poly	ab1791
H3ac	Millipore (Burlington, MA, USA)	17	Rabbit	poly	06-599
H4ac	Millipore (Burlington, MA, USA)	10	Rabbit	poly	06-598
H3K9me2	ACTIVE MOTIF (Tokyo, Japan)	17	Rabbit	poly	39753
H3K27me2	ACTIVE MOTIF (Tokyo, Japan)	17	Rabbit	poly	39245/6
H3K27me3	Millipore (Burlington, MA, USA)	17	Rabbit	poly	07-449
Horseradish peroxidase-conjugated Goat anti-mouse IgG	Jackson ImmunoResearch (West Grove, PA, USA)	/	Goat	poly	115-035-003
Horseradish peroxidase-conjugated Goat anti-rabbit IgG	Jackson ImmunoResearch (West Grove, PA, USA)	/	Goat	poly	111-035-144

Appendix Table 2. Primer sequences used for PCR (RT-qPCR, real-time quantitative PCR; ChIP, chromatin immunoprecipitation; BSP, bisulfite sequencing PCR)

Primer name	Sequence	Notes
RalGAPα1	5'-CTCCTACCCAGAGATTCTACCCA-3' (forward) 5'-CATGTTATGGCAGACACATGAAGGC-3' (reverse)	RT-qPCR
RalGAPα2	5'-AGAACGTTTCATCTTCAGGCTCT-3' (forward) 5'-AGGGTTGAGTTATTTGCTGCCTA-3' (reverse)	
RalGAPβ	5'-CTCAGTTAAACACGTGCATTGGT-3' (forward) 5'-CAACTGAGTAGAAGGCTGTGACT-3' (reverse)	
RalGDS	5'-GAGATGAACCCCAAGAGAG-3' (forward) 5'-CTTCTTGGTCCTGAGGGTGT-3' (reverse)	
RGL1	5'-CAAGCCCAAACTGTGAAGAA-3' (forward) 5'-AGCACGTGAATTCTGCTGAC-3' (reverse)	
RGL2	5'-TTCAGTTTATGCCGTGGTGT-3' (forward) 5'-CCACGACATTCATTCTGGAG-3' (reverse)	
RGL3	5'-CCTGCAATCTAACCCCATCT-3' (forward) 5'-ATCTCCCACTCCTTCCTCCT-3' (reverse)	
RALGPS1	5'-AGGGGCCTCTGAGAAGAAAA-3' (forward) 5'-GAAATCGGGAACCAGTCTGA-3' (reverse)	
RALGPS2	5'-TTGTGTGGGACACAGCTTTT-3' (forward) 5'-AGGCTGCACTCAAATGCTTA-3' (reverse)	
GAPDH	5'-GAAGGTGAAGGTCGGAGTC-3' (forward) 5'-GAAGATGGTGATGGGATTTC-3' (reverse)	
RalGAPα2 Region 1	5'-CCCTTCCTACAAAGAGGCAAGAT-3' (forward) 5'-AAATGAGTTGCTTTGGCACTAGG-3' (reverse)	RT-qPCR for CHIP
RalGAPα2 Region 2	5'-CCCTTGTGTGAATCCAGAAGCTA-3' (forward) 5'-CATTTTCCTCTAGTGCAACGTGA-3' (reverse)	
RalGAPα2 Region 3	5'-CCTATGCTTTGATTCGCGTGG-3' (forward) 5'-CTTCTGGGTGGACTTCTTCACAT-3' (reverse)	
RalGAPα2 BSP1	5'-TGACACTTTTCTTACTGAGATTTTGG-3' (forward) 5'-AGACAGTCCTCCAATCAGGCTGG-3' (reverse)	Bisulfite sequencing PCR
RalGAPα2 BSP2	5'-CCAGCCTGATTGGAGGACTGT-3' (forward) 5'-CTTCTGGGTGGACTTCTTCACATCC-3' (reverse)	
RalGAPα2 BSP3	5'-CTGAAAAAGCTGAAAGGATGTCAA-3' (forward) 5'-AGAGTCCTCCAATCAGGCTGG-3' (reverse)	
RalGAPα2 1	5'-AAGATAGTTGTGTTGTTTTAATTTGGATGGAA-3' (forward) 5'-CTTATTCCCTAAAACAAAACTTTAAACTAAAAA-3' (reverse)	NGS-BSP
RalGAPα2 2	5'-TTTTTAGTTTAAAGTTTTGTTTTAGGGAATAAG-3' (forward) 5'-CCTAAATTCCTAAAACCCAACCTCACT-3' (reverse)	
RalGAPα2 3	5'-AGTGAGGTTGGGTTTTAGGAATTTAGGG-3' (forward) 5'-CCCAAAAATCTCAATAAAAAAAATATCAAAAC-3' (reverse)	
M13-M4 M13-RV	5'-GTTTTCCAGTCACGAC-3' 5'-CAGGAAACAGCTATGAC-3'	TA-cloning PCR
HRAS	5'-AGTCGCGCCTGTGAACG-3' (forward) 5'-TTGCTTCCGTCCTTCCTTCC-3' (reverse)	PCR for *RAS* mutation detection
KRAS	5'-CATTTCGGACTGGGAGCGAG-3' (forward) 5'-ACTCTGGGAATACTGGCACTTAG-3' (reverse)	
NRAS	5'-CCCGGCTGTGGTCCTAAATC-3' (forward) 5'-GAAGTCAGGACCAGGGTGTC-3' (reverse)	

Appendix Table 3. RAS mutation status in eight OSCC cell lines.

Cell Lines	**SNP**	**AA Mutation**	**SNP**	**AA Mutation**	**SNP**	**AA Mutation**
	HRAS	*HRAS*	*NRAS*	*NRAS*	*KRAS*	*KRAS*
HSC-2	wild	wild	wild	wild	wild	wild
HSC-3	wild	wild	wild	wild	wild	wild
OSC19	H27H hetero, CAT→CAC	wild	wild	wild	wild	wild
OSC20	H27H homo, CAT→CAC	wild	wild	wild	wild	wild
Ca9-22	wild	wild	wild	wild	wild	wild
HOC313	**G12S homo, GGC→AGC**	**G12S homo**	wild	wild	wild	wild
SAS	H27H hetero, CAT→CAC	wild	wild	wild	wild	wild
TSU	wild	wild	wild	wild	wild	wild

Amino acid mutations in hot spots, including G12, G13, A59, Q61, K117, A146 in HRAS, NRAS, and KRAS were evaluated.

One active mutation in HRAS (G12S) was found in HOC313 cells.

SNP, single nucleotide polymorphism

Appendix Table 4.

Clinicopathologic characteristics of patients (n=116) showing low and high expression of RalGAPα2

Characteristics	n (%)	RalGAPα2 expression		*P*
		Low	High	
Gender				
Male	66(57)	42	24	
Female	50(43)	23	27	0.0581
Age (y)				
<60	61(53)	36	25	
≥60	55(47)	29	26	0.4956
Pathologic stage				
Ⅰ, Ⅱ	112(97)	61	51	
Ⅲ,Ⅳ	4(3)	4	0	0.0714
T stage				
T_{1-2}	73(63)	42	31	
T_{3-4}	43(37)	23	20	0.6715
Lymph node metastasis				
Negative	86(74)	46	40	
Positive	30(26)	19	11	0.3496

1. Appendix experimental procedures.

Materials and reagents

Stock solutions of 5-aza-2'-deoxycytidine (5-aza-2'-dc; Abcam, Cambridge, UK), trichostatin A (TSA; Wako Pure Chemical Industries, Osaka, Japan) and GSK-126 (Adooq BioScience, Irvine, CA, USA) were prepared using distilled water, ethanol and dimethylsulfoxide respectively. Antibodies and primers used are listed in Appendix Tables 1 and 2, respectively. This study was approved by the Medical Ethics Committee of West China Hospital of Stomatology, Sichuan University (WCHSIRB-ST-2016-153) and the Ethics Committee of Tohoku University (2017-3-020). Patient samples were collected after obtaining informed consents.

Cell culture

The human OSCC cell lines, OSC19, OSC20, TSU and HOC313 were generated as previously described (Ishisaki et al. 1994; Yokoi 1988; 1990). HSC-2, HSC-3, SAS and Ca9-22 OSCC cell lines were obtained from the RIKEN BioResource Center (Ibaraki, Japan). All cells were cultured using High Glucose Dulbecco's modified Eagle medium (DMEM; Nacalai Tesque, Kyoto, Japan) supplemented with 10% fetal bovine serum (FBS; Biological Industries, Cromwell, CT, USA) and 1% Penicillin-Streptomycin Mixed Solution (Nacalai Tesque) at 37°C in a humid incubator with 5% CO_2.

Pull-down assay analyzing Ral activation states

The pull-down assay was performed as previously described (Saito et al. 2013). Briefly, cell extracts were prepared from cells stimulated using 10% FBS for 5 min at 37°C after serum starvation and pull down was performed with the Ral-binding domain of Sec5 that bound exclusively GTP-bound active Ral.

Co-immunoprecipitation assay

Co-immunoprecipitation (Co-IP) was carried out by incubation of cell lysate (100 μg of protein) with anti-RalGAPα1, anti-RalGAPα2, or control IgG-conjugated protein G-sepharose beads overnight at 4°C. Bead-associated proteins were subjected to western blot analysis.

Real-time quantitative polymerase chain reaction (RT–qPCR) analysis

Normal epithelia and paired cancer tissues from 30 patients were obtained from Head and Neck Oncology of West China Hospital of Stomatology, Sichuan University. Total RNA from cultured cells and tissues was extracted using an Isospin Cell & Tissue RNA kit (NIPPON GENE, Toyama, Japan) and cDNA synthesized using a ReverTra Ace kit (TOYOBO, Osaka, Japan). RT–qPCR was performed using SYBR Premix Ex Taq™ II kit (TaKaRa, Kyoto, Japan) according to the manufacturer's instructions. Results were normalized to a reference gene, glyceraldehyde-3-phosphate dehydrogenase (*GAPDH*), and calculated using a $2^{-\Delta C_T}$ or $2^{-\Delta\Delta C_T}$ method (Schmittgen and Livak 2008).

Small interfering RNA treatment

Cells were transfected with three predesigned small interfering RNAs (siRNAs, 10 nM; Ambion, Thermo Fisher Scientific, Waltham, MA, USA) using Lipofectamine RNAiMAX (Invitrogen, Waltham, MA, USA) according to the manufacturers' instructions. Cells transfected with an optimal siRNA for 48 h were used for experiments.

Lentiviral infection

TSU cells infected with lentivirus to express RalGAPα2 or mutant RalGAPα2-N1742K were prepared as previously described (Saito et al. 2013). After incubation at 37°C for 48 h, infected cells were selected using blasticidin (5 μg/mL, Invitrogen) for 48 h. Stably RalGAPα2- or mutant RalGAPα2-N1742K-expressing cells were used for experiments.

Migration assay

The confluent cells were scratched and incubated in serum-free DMEM for the indicated periods. Photographs were taken using a BZ-9000E microscope (KEYENCE Corp, Japan), as described previously (Saito et al. 2013). Each area lacking cells was measured using Image J (https://imagej.nih.gov/ij/) and a migration index was calculated using the following formula: 1−(area after 36 h or 24 h / area at the beginning).

Matrigel transwell invasion assay

For siRNA-RalGAPβ and RalGAPα2 expression assays, 3×10^5 HSC-2 cells incubated for 24 h or 5×10^4 TSU cells incubated

for 16 h were analyzed as previously described (Tanaka et al. 2012; Yoshida et al. 2014).

Immunohistochemistry

Samples from 116 patients with OSCC were evaluated. Immunostaining and analyses were performed as described previously (Saito et al. 2013).

The Cancer Genome Atlas (TCGA) analysis

Gene expression RNAseq data (version 2017-10-13) and clinical data (version 2016-04-27) from TCGA Head and Neck Cancer (HNSC) project were retrieved from UCSC-Xena (https://tcga.xenahubs.net; Goldman M, et al). Samples of OSCC tissues (n=342) were analyzed for gene expression and clinical traits after removing normal tissue samples, samples of other types of HNSC or unshared samples. The prognostic values of RALGAPα2 were analyzed in an R/Bioconductor environment. Patients (n=286) with recurrence-free survival (RFS) data or patients (n=339) with overall survival data were subjected to perform Kaplan-Meier analysis respectively.

Bisulfite sequencing analysis

HSC-2 and TSU cells (1×10^5) treated with or without 5-aza-2'-dc (0.5 μM) for 96 h were collected and subjected to DNA isolation and bisulfite treatment using the EpiTect Plus DNA Bisulfite Kit (QIAGEN, Hilden, Germany) following the manufacturer's protocol. Converted DNA was amplified by PCR using an EpiTaq HS Kit (TaKaRa). PCR amplicons were purified and cloned using a

Mighty TA-cloning Kit (TaKaRa) based on the manufacturer's instructions. Sequencing data were analyzed using QUMA (http://quma.cdb.riken.jp/; Kumaki et al. 2008).

Next generation sequencing-bisulfite sequencing PCR (NGS-BSP) analysis

The DNA methylation levels of the RalGAPα2 promoter region in normal epithelium and paired cancer tissues from six patients were assessed by next generation bisulfite sequencing according to a previously published method (Gao et al. 2015; Gao et al. 2014a; Gao et al. 2014b; Pan et al. 2018). In brief, primers for genomic amplification were designed using the online MethPrimer software (Appendix Table 2). Genomic DNA (1 μg) was converted using the ZYMO EZ DNA Methylation-Gold Kit (Zymo Research, Irvine, CA, USA) and used as templates for PCR amplification using KAPA 2G Robust HotStart PCR Kit (Kapa Biosystems, Wilmington, MA, USA). For each sample, PCR products were pooled equally, 5'-phosphorylated, 3'-dA-tailed and ligated to a barcoded adapter using T4 DNA ligase (New England Biolabs, Ipswich, MA, USA). Barcoded libraries from all samples were sequenced on an Illumina platform by Shenzhen Acegen Technology Co.，Ltd.

Chromatin immunoprecipitation (ChIP)

The method used for the ChIP assay referred to the protocol of Nelson et al. (Nelson et al. 2006). Briefly, a total of 1×10^7 HSC-2 or TSU cells, treated with or without TSA (0.1 μM, 24 h) or GSK-126 (0.5 μM, 96 h), were cross-linked using 1% formaldehyde and quenched by 125 mM glycine. The cell lysates were treated with micrococcal nuclease (New England Biolabs) at 37°C for 20 min and

the reaction was stopped by EDTA, followed by sonication. The nuclear lysates were incubated with the indicated antibodies at 4°C for 1 h. Antibody-associated DNA was then collected by Protein A/G Magnetic Beads (Thermo Fisher Scientific) followed by elution with a ChIP direct elution buffer at 65°C for 4 h. Following treatment with RNase and proteinase K, the DNA was purified using a ChIP DNA Clean & Concentrator Kit (ZYMO Research). The DNA was subjected to RT-qPCR analysis as described above.

RAS mutation detection

Mutations in *HRAS*, *KRAS*, and *NRAS* genes were analyzed in oral cancer cell lines (HSC-2, HSC-3, OSC19, OSC20, Ca9-22, HOC313, SAS, and TSU) by their cDNA sequences. Total RNA was isolated from sub-confluent cells using an ISOSPIN Cell & Tissue RNA Kit (NIPPON Gene, Toyama, Japan). The cDNA was prepared by reverse transcription using the ReverTra Ace qPCR Master Mix (TOYOBO, Osaka, Japan). DNAs of *HRAS*, *KRAS*, and *NRAS* were amplified by PCR using KOD Fx Neo (TOYOBO) with primers listed in Appendix Table 2. The PCR products were purified and sequenced using a BigDye Terminator v3.1 Cycle Sequencing Kit using a 3130 Genetic Analyzer (both from Beckman Coulter, Brea, CA, USA). Coding sequences, including hot spots of mutations such as G12, G13, A59, Q61, K117, A146, were evaluated.

Cell proliferation assay

Confluent cells (1×10^5), prepared as described above, were resuspended in complete medium, seeded in a 6-well plate in triplicate and incubated for 24, 48, 72 or 96 h. The cell proliferation rate was evaluated by cell counting using a Z1 COULTER

(Beckman Coulter).

Soft agar colony formation assay

Confluent cells (1×10^5), prepared as described above, were mixed with 0.36% agar and seeded in a 6-well plate coated with 0.75% agar. Cells were cultured for 2 weeks. Colonies were captured in six randomly selected fields in triplicate using a BZ-9000E microscope and counted by Image J.

Statistical analysis

A two-tailed unpaired Student's *t*-test was used for each comparison between two groups. One-way ANOVA followed by Tukey's multiple comparison test was performed for comparisons among three or more groups. Two-way ANOVA was performed to analyze the significance of data with multiple variates. A ratio paired *t*-test was performed for the comparison of RalGAPα2 mRNA expression in normal epithelial and cancer tissues. A Chi-square test was performed to analyze clinicopathological characteristics between patients with high and low expression of RalGAPα2 in the OSCC tissues. Overall survival and recurrence-free survival were evaluated by the Kaplan-Meier analysis, and the significance was calculated by log-rank test. A paired *t*-test was performed for a comparison of methylation level of cytosines followed by guanine residues (CpGs) within RalGAPα2 promoter. A P value < 0.05 was considered statistically significant.

Appendix Figure 1

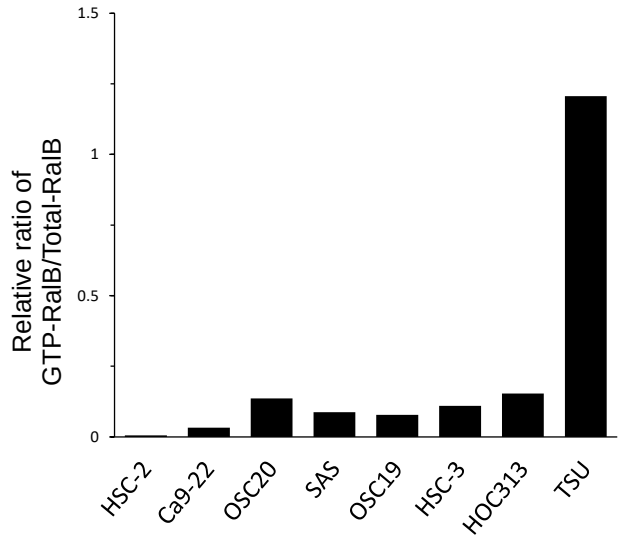

Appendix Figure 1. Ratios of GTP-RalB to total-RalB. Ratios of GTP-RalB to total-RalB calculated by the quantification of data in Fig. 1C.

Appendix Figure 2

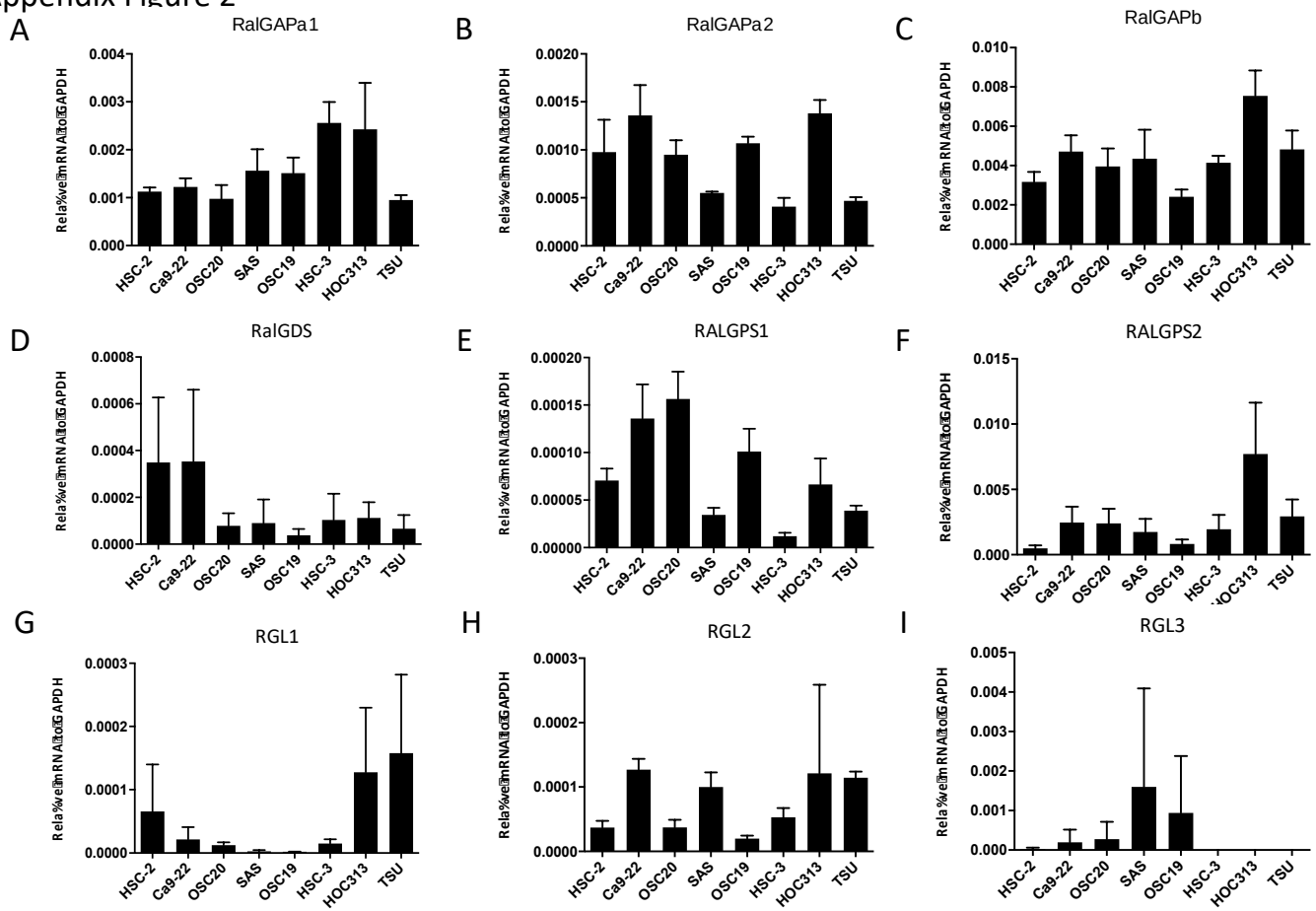

Appendix Figure 2. mRNA levels of RalGAPs and RalGEFs. (A-I) RT-qPCR was used to measure mRNA levels of RalGAPa1 (A), RalGAPa2 (B), RalGAPb (C), RalGDS (D), RalGPS1 (E), RalGPS2 (F), RGL1 (G), RGL2 (H) and RGL3 (I) relative to GAPDH in oral squamous cell carcinoma (OSCC) cell lines.

Appendix Figure 3

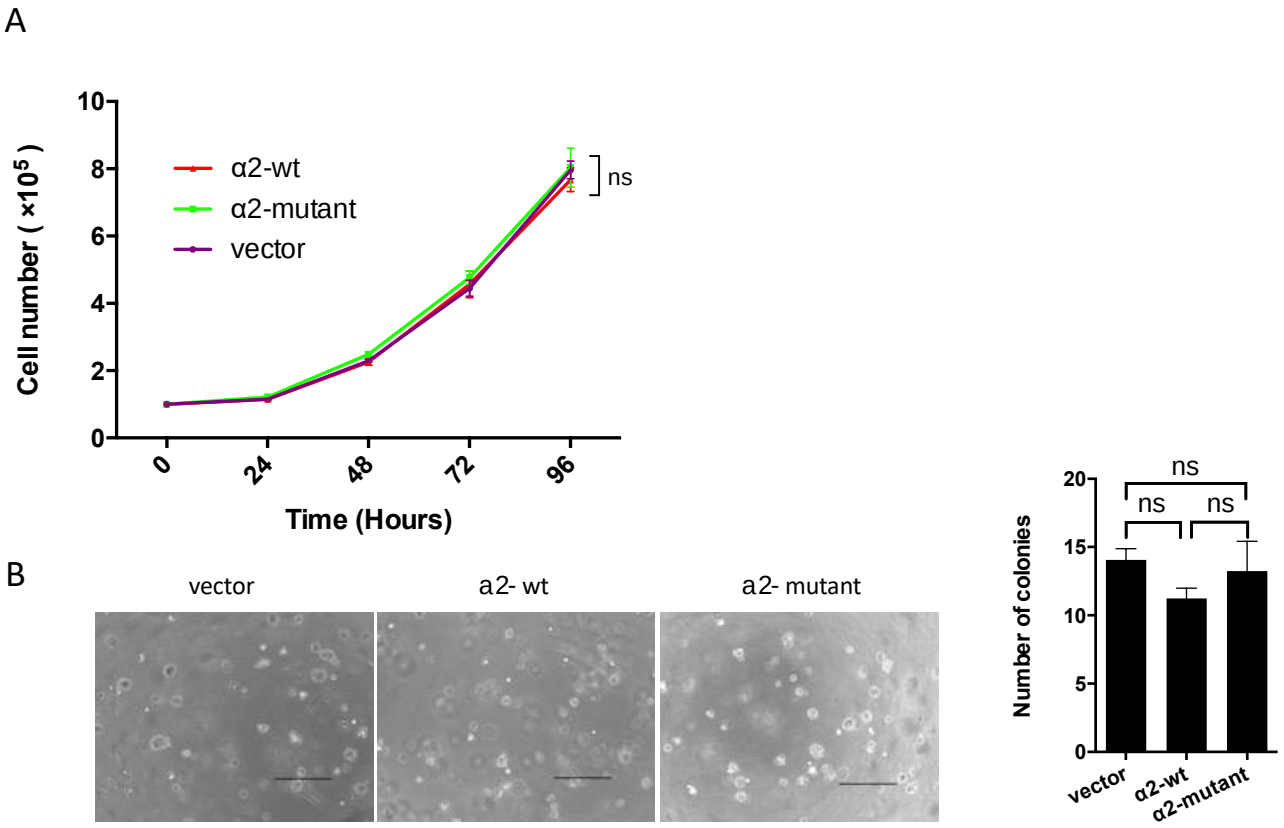

Appendix Figure 3. The effect of RalGAP on the growth of TSU OSCC cells. (A) Cell numbers were counted to evaluate the proliferation rate of TSU cells. The cells stably expressing wild-type-RalGAPa2 (a2-wt) and RalGAPa2 N1742K (a2-mutant), and treated with vector were seeded at 1 x 10^5 cells/well. At 24, 48, 72, and 96 h after plating, cell numbers were measured. (B) A soft agar colony formation assay was used to investigate the anchorage-independent growth of TSU cells stably expressing a2-wt and a2-mutant, and treated with the vector alone. The scale bars represent 300 μm. The right histogram shows a quantitative analysis.

Appendix Figure 4

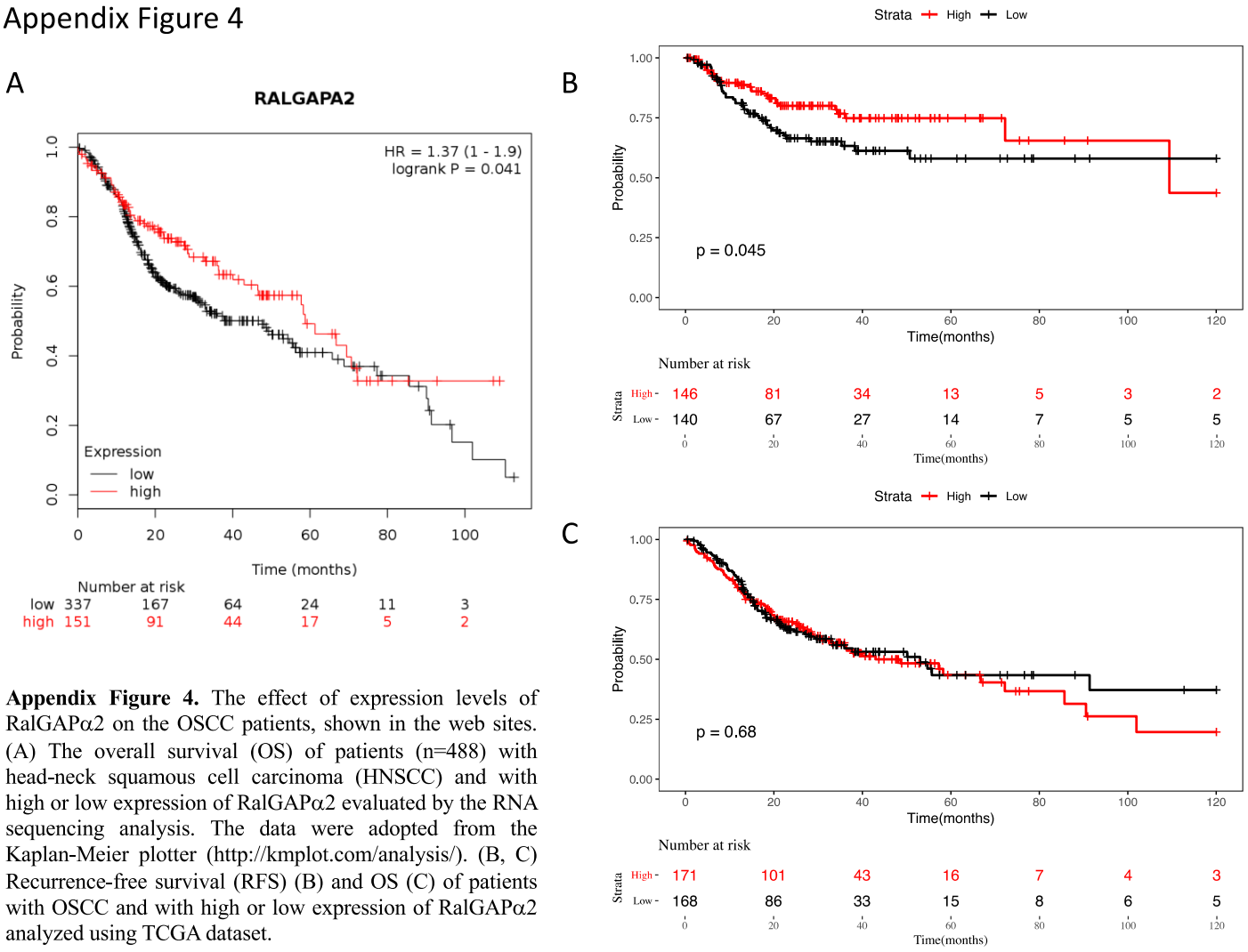

Appendix Figure 4. The effect of expression levels of RalGAPα2 on the OSCC patients, shown in the web sites. (A) The overall survival (OS) of patients (n=488) with head-neck squamous cell carcinoma (HNSCC) and with high or low expression of RalGAPα2 evaluated by the RNA sequencing analysis. The data were adopted from the Kaplan-Meier plotter (http://kmplot.com/analysis/). (B, C) Recurrence-free survival (RFS) (B) and OS (C) of patients with OSCC and with high or low expression of RalGAPα2 analyzed using TCGA dataset.

Appendix Figure 5

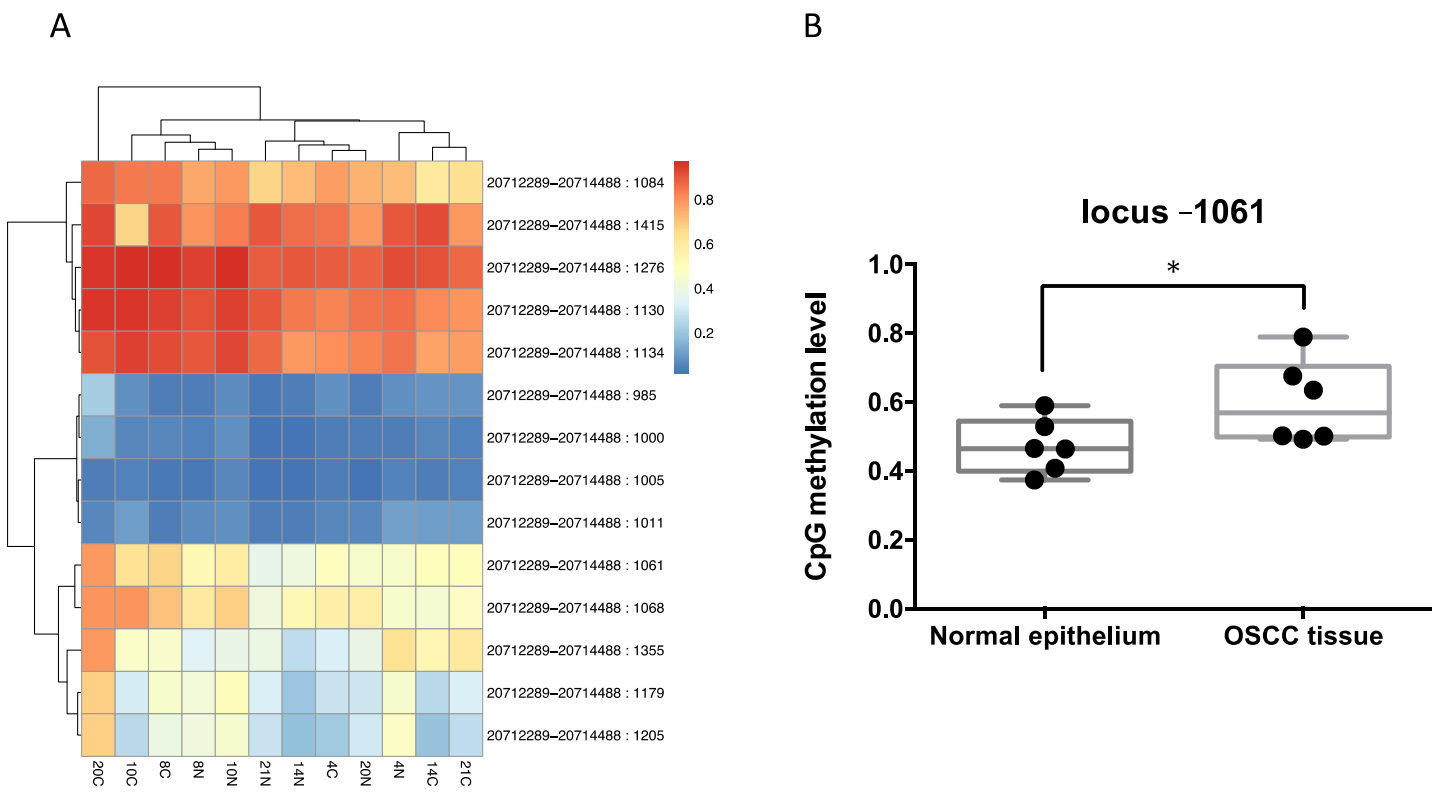

Appendix Figure 5. Comparison of DNA methylation in the promotor region of RalGAPα2 between OSCC and adjacent normal tissues. (A) Heat map depicting the hierarchical clustering of 14 differentially methylated CpGs of the RalGAPα2 promoter between -1201 and -705 in six-paired OSCC tissues and normal epithelia. Red color, high methylation rate; white color, moderate methylation rate; blue color, low methylation rate. C indicates OSCC tissue samples, and N indicates adjacent normal epithelia. (B) The methylation level of CpG locus–1061 of RalGAPα2 promoter in six OSCC samples in comparison with paired normal epithelia. The y-axis indicates probability of methylation of the CpG. *$P < 0.05$.

Appendix Figure 6

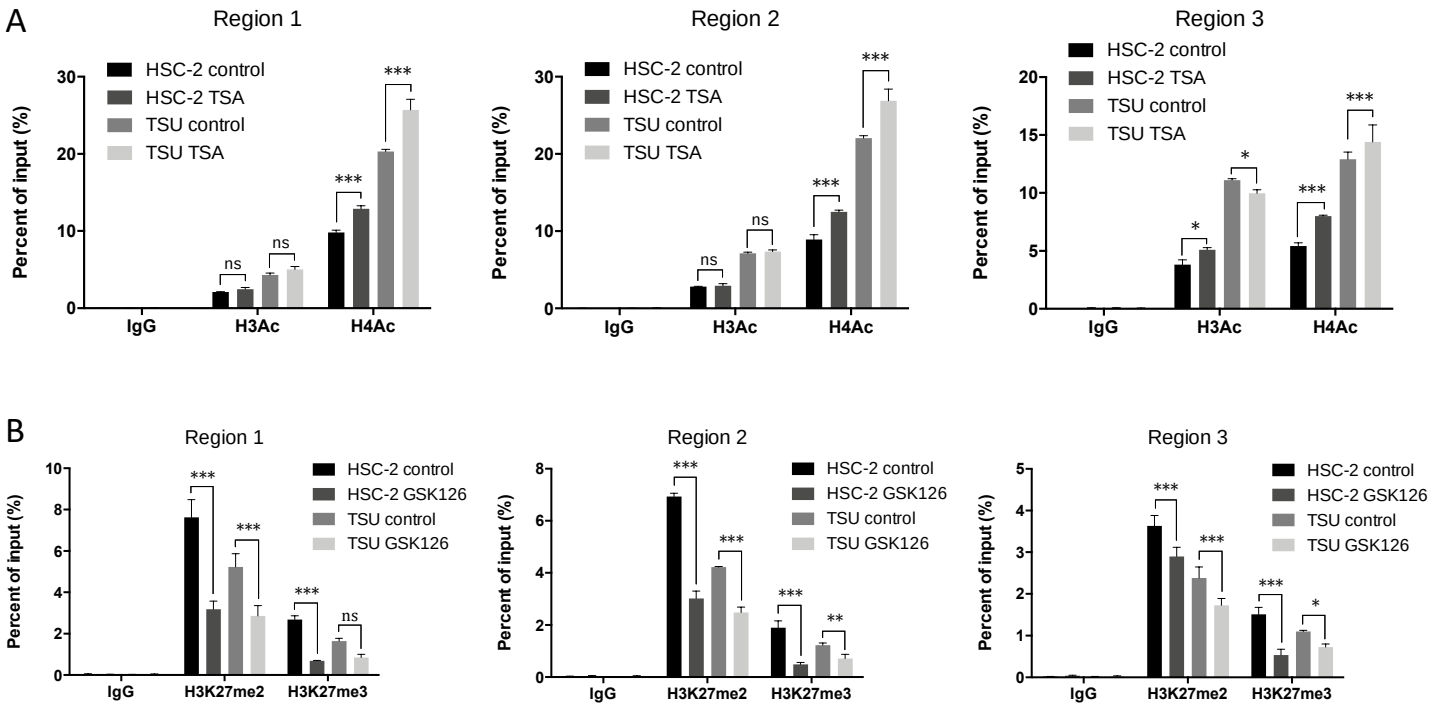

Appendix Figure 6. The effect of TSA and GSK 126 on the histone modification in the *RalGAP*a*2* promoter in HSC-2 and TSU OSCC cells. (A) HSC-2 and TSU cells were treated with TSA (0.1 μM) for 24 h. Modifications of H3Ac and H4Ac within the *RalGAP*a*2* promoter (three regions) were analyzed by ChIP analysis. (B) HSC-2 and TSU cells were treated with 0.5 μM GSK-126 for 96 h. Modifications of H3K27me2 and H3K27me3 within the *RalGAP*a*2* promoter (three regions) were analyzed by the ChIP analysis. In (A) and (B), rabbit IgG served as a negative control for immunoprecipitation. Data are expressed as percentage of the input.

Appendix Figure 7

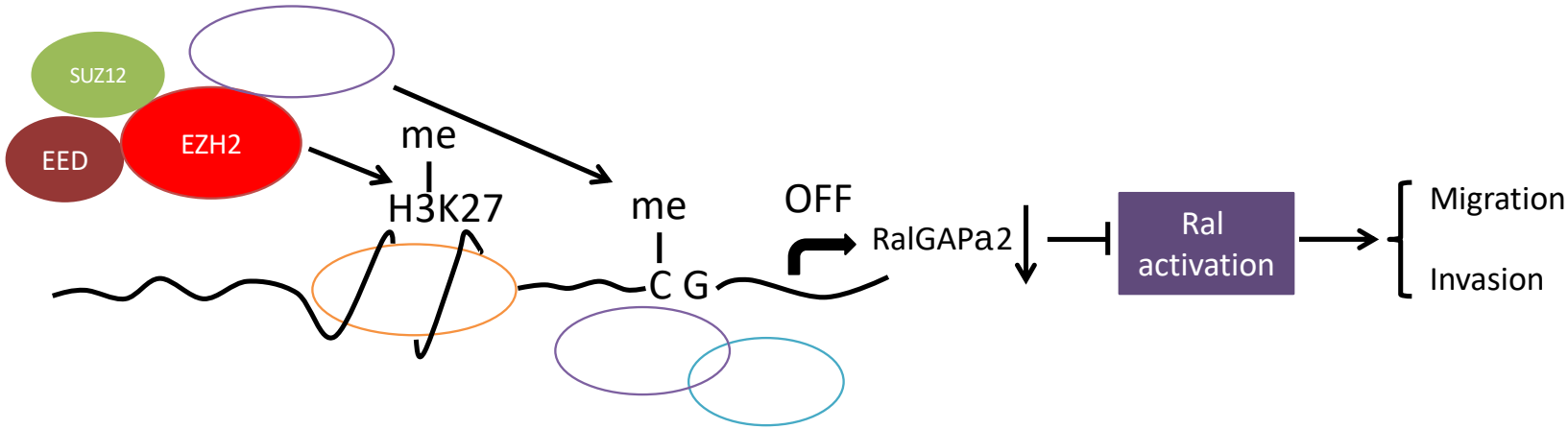

Appendix Figure 7. A model of epigenetic control of RalGAPa2 expression. The carcinogenesis of RalA activation in OSCC may result from RalGAPa2 downregulation induced by a crosstalk epigenetic modification, including DNA methylation, histone acetylation and histone methylation. EZH2: Enhancer of zeste homologue 2; EED: embryonic ectoderm development; SUZ12: suppressor of zeste 12; DNMTs: DNA methyltransferases; MeCP2: methyl CpG binding protein 2; HDAC: histone deacetylase.

Appendix References

Gao F, Liang H, Lu H, Wang J, Xia M, Yuan Z, Yao Y, Wang T, Tan X, Laurence A, et al. 2015. Global analysis of DNA methylation in hepatocellular carcinoma by a liquid hybridization capture-based bisulfite sequencing approach. Clin Epigenet. 7:86.

Gao F, Xia Y, Wang J, Lin Z, Ou Y, Liu X, Liu W, Zhou B, Luo H, Zhou B et al. 2014a. Integrated analyses of DNA methylation and hydroxymethylation reveal tumor suppressive roles of ECM1, ATF5, and EOMES in human hepatocellular carcinoma. Genome Biol. 15(12):533.

Gao F, Zhang J, Jiang P, Gong D, Wang JW, Xia Y, Ostergaard MV, Wang J, Sangild PT. 2014b. Marked methylation changes in intestinal genes during the perinatal period of preterm neonates. BMC Genomics. 15:716.

Ishisaki A, Oida S, Momose F, Amagasa T, Rikimaru K, Ichijo H, Sasaki S. 1994. Identification and characterization of autocrine-motility-factor-like activity in oral squamous-cell-carcinoma cells. Int J Cancer. 59(6):783–788.

Kumaki Y, Oda M, Okano M. 2008. QUMA: quantification tool for methylation analysis. Nucleic Acids Res. 36(Suppl 2):W170–W175.

Nelson JD, Denisenko O, Bomsztyk K. 2006. Protocol for the fast chromatin immunoprecipitation (ChIP) method. Nat Protoc. 1(1):179–185.

Pan X, Gong D, Nguyen DN, Zhang X, Hu Q, Lu H, Fredholm M, Sangild PT, Gao F. 2018. Early microbial colonization affects DNA methylation of genes related to intestinal immunity and metabolism in preterm pigs. DNA Res. 25(3):287–296.

Schmittgen TD, Livak KJ. 2008. Analyzing real-time PCR data by the comparative C_T method. Nat Protoc. 3(6):1101–1108.

Tanaka T, Nakayama H, Yoshitake Y, Irie A, Nagata M, Kawahara K, Takamune Y, Yoshida R, Nakagawa Y, Ogi H, et al. 2012. Selective inhibition of nuclear factor-κB by nuclear factor-κB essential modulator-binding domain peptide suppresses the metastasis of highly metastatic oral squamous cell carcinoma. Cancer Sci. 103(3):455–463.

Yokoi T. 1990. Some properties of a newly established human cell line derived from an oral squamous carcinoma. Tumor Res. 25:93–103.

Yokoi T, Homma H, Odajima T. 1988. Establishment and characterization of OSC19 cell line in serum-and protein-free culture. Tumor Res. 24:1–17.

Yoshida R, Nakayama H, Nagata M, Hirosue A, Tanaka T, Kawahara K, Nakagawa Y, Matsuoka Y, Sakata J, Arita H, et al. 2014. Overexpression of nucleostemin contributes to an advanced malignant phenotype and a poor prognosis in oral squamous cell carcinoma. Br J Cancer. 111(12):2308–2315.